Letter

How well does nonrelativistic QCD factorization work at next-to-leading order?

Nora Brambilla,[1,2,3] Mathias Butenschoen,[4] and Xiang-Peng Wang[5,1,*]

[1]*Technical University of Munich, TUM School of Natural Sciences, Physics Department, James-Franck-Strasse 1, 85748 Garching, Germany*

[2]*Technical University of Munich, Institute for Advanced Study, Lichtenbergstrasse 2a, 85748 Garching, Germany*

[3]*Technical University of Munich, Munich Data Science Institute, Walther-von-Dyck-Strasse 10, 85748 Garching, Germany*

[4]*II. Institut für Theoretische Physik, Universität Hamburg, Luruper Chaussee 149, 22761 Hamburg, Germany*

[5]*Institute of Particle Physics and Key Laboratory of Quark and Lepton Physics (MOE), Central China Normal University, Wuhan, Hubei 430079, China*

(Received 18 November 2024; accepted 5 May 2025; published 15 July 2025)

We perform a thorough investigation of the universality of the long-distance matrix elements (LDMEs) of nonrelativistic QCD factorization based on a next-to-leading order (NLO) fit of J/ψ color octet LDMEs to high transverse momentum p_T J/ψ and η_c production data at the LHC. We thereby apply a novel fit-and-predict procedure to systematically take into account scale variations, and predict various observables never studied in this context before. In particular, the LDMEs can well describe J/ψ hadroproduction up to the highest measured values of p_T, as well as $\Upsilon(nS)$ production via potential nonrelativistic QCD based relations. Furthermore, J/ψ production in $\gamma\gamma$ and γp collisions is surprisingly reproduced down to $p_T = 1$ GeV, as long as the region of large inelasticity z is excluded, which may be of significance in future quarkonium studies, in particular at the EIC and the high-luminosity LHC. In addition, our summary reveals an interesting pattern as to which observables still evade a consistent description.

DOI: 10.1103/8xqs-45pz

Introduction and overview. The hierarchy of energy scales $m_Q \gg m_Q v \gg m_Q v^2$ makes heavy quarkonium production an ideal laboratory to study both the perturbative and nonperturbative aspects of QCD. Here, m_Q stands for the heavy quark mass and v for the relative velocity of the heavy quark and antiquark in the rest frame of the quarkonium. The most prominent approach to describe quarkonium production and decay is via nonrelativistic QCD (NRQCD) [1]. This is an effective field theory that comes with a conjectured factorization formula, according to which a quarkonium, H, production cross section factorizes into perturbatively calculable short-distance coefficients (SDCs) and universal nonperturbative long-distance matrix elements (LDMEs) $\langle \mathcal{O}^H(n) \rangle$, where $n = {}^{2S+1}L_J^{[1/8]}$ denotes an intermediate color singlet ($^{[1]}$, CS) or octet ($^{[8]}$, CO) heavy quark-antiquark state with spin S, orbital angular momentum L, and total angular momentum J. NRQCD predicts the LDMEs to scale with certain powers of v^2 via velocity scaling rules [2]. These rules predict the leading (next-to-leading) v^2 contributions to stem for $\psi(nS)$ and $\Upsilon(nS)$ production from $n = {}^3S_1^{[1]}$ ($^1S_0^{[8]}$, $^3S_1^{[8]}$, $^3P_J^{[8]}$) and for η_c production from $n = {}^1S_0^{[1]}$ ($^3S_1^{[8]}$, $^1S_0^{[8]}$, $^1P_1^{[8]}$). The LDMEs are, however, not all independent. Up to corrections of order v^2, the LDMEs of J/ψ and η_c are mutually related via heavy quark spin symmetry (HQSS) [1], and the various $\psi(nS)$ and $\Upsilon(nS)$ LDMEs by relations [3,4] based on potential NRQCD (pNRQCD) [5–9].

To scrutinize the LDME universality is an ongoing task. Currently, these tests are performed at next-to-leading order (NLO) in the strong coupling constant α_s, and may, for LDMEs concerning J/ψ, be summarized as follows: The LDMEs of the global fit [10] to 194 points of J/ψ production data in pp, $p\bar{p}$, γp, $\gamma\gamma$, and e^+e^- scattering describe the fitted observables reasonably well, but result in discrepancies for η_c [11] and $J/\psi + W$ or Z [12] yields at the LHC, and predict strong transverse J/ψ polarization, not observed at Tevatron or the LHC [13]. All other LDME fits are restricted to high transverse momentum p_T

*Contact author: xpwang@ccnu.edu.cn

Published by the American Physical Society under the terms of the Creative Commons Attribution 4.0 International license. Further distribution of this work must maintain attribution to the author(s) and the published article's title, journal citation, and DOI. Funded by SCOAP³.

hadroproduction data, with low-p_T cuts of typically 7 GeV or higher [3,4,14–18]. They are successful at describing the fitted high p_T yields and the measured J/ψ polarization, but describe neither the hadroproduction data at lower p_T nor the inelasticity variable z integrated photoproduction [19], and the $J/\psi + W$ or Z data [20–22] at best marginally [12]. η_c hadroproduction is almost exclusively determined by $\langle \mathcal{O}^{J/\psi}({}^1S_0^{[8]})\rangle$. The fit results of Refs. [3,4,14] leave $\langle \mathcal{O}^{J/\psi}({}^1S_0^{[8]})\rangle$ poorly constrained, predicting η_c production therefore only with very large uncertainties. On the other hand, Refs. [15,18] lead to an overshoot of η_c data. Only analyses [16,17] describe η_c production well, because they use LHCb η_c data directly as input to constrain $\langle \mathcal{O}^{J/\psi}({}^1S_0^{[8]})\rangle$. The latter approach thus appears to be the most promising fit strategy, and is the one we adopt here.

In our NLO analysis, we fit the three J/ψ CO LDMEs to prompt LHCb η_c [23,24] and CMS J/ψ [25] production yields, the latter data ranging from $p_T = 10$ to 120 GeV. After showing that these LDMEs lead to a good description of the CMS J/ψ polarization data [25], we go on to make predictions for observables never studied in this context before: We show that our LDMEs can predict well recent ATLAS J/ψ hadroproduction data with p_T ranging up to 360 GeV [26]. We further show that, contrary to common perceptions, these fits can well describe $\gamma\gamma$ scattering at LEP [27] and J/ψ photoproduction at HERA [28,29] even at p_T as low as 1 GeV, as long as we consider the region $z < 0.6$. Even $\Upsilon(nS)$ production [30] is well reproduced, while $J/\psi + Z$ production [21] remains intricate to be interpreted. All these findings are nontrivial tests of NRQCD factorization never performed before.

A technological advancement is our consistent fit-and-predict procedure which systematically takes into account the effect of scale variations, the largest source of SDC uncertainty. In most NRQCD analyses, e.g., Refs. [14–17], scale variations are completely ignored. In Refs. [10–13,19,31–35], scale uncertainties are considered in predictions and plots, but, unrealistically, assumed to be uncorrelated to the LDME errors. In analyses [3,4,18], scale uncertainties are treated as global theory errors in the fits, unable, however, to predict scale uncertainties of other observables with own individual scale dependencies. We therefore proceed as follows. We do three separate fits, with the renormalization and factorization scales μ_r and μ_f set equal and equal to $\mu_0/2$, μ_0, and $2\mu_0$, respectively, with μ_0 our default hard scale. For prediction plots, we then create three error bands, each created using the LDME uncertainties of one fit, in combination with the SDCs evaluated with the respective scale choice. Our overall uncertainty is then the envelope of the three error bands created this way.

Details and input of the calculation. We calculate the SDCs needed for hadroproduction yields using the dipole subtraction based codes described in Refs. [12,36,37]. For J/ψ polarization and for J/ψ production in γp and $\gamma\gamma$ scattering, we calculate the SDCs using the phase-space slicing [38] based codes described in Refs. [10,13,37,39]. We use three (four) light quark flavors for charmonia (bottomonia) in loops and external legs, heavy quarks only for the outgoing $Q\bar{Q}$ pair. We set the default hard scale to be $\mu_0 = m_T = (p_T^2 + 4m_Q^2)^{1/2}$, the quarkonium transverse mass, and the NRQCD scale to be $\mu_\Lambda = m_Q$. We choose the on-shell charm and bottom masses to be $m_c = 1.5$ GeV and $m_b = 4.75$ GeV. As proton parton distribution function (PDF) set, we use CTEQ6M [40], and for $\alpha_s(\mu_r)$ correspondingly the two loop running formula with the asymptotic scale parameter $\Lambda_{\rm QCD}^{(n_f=4)} = 326$ MeV ($\Lambda_{\rm QCD}^{(n_f=5)} = 226$ MeV) for charmonia (bottomonia). In γp and $\gamma\gamma$ scattering, we use the Weizsäcker-Williams approximation for the photon flux and for resolved photons the AFG04_BF PDF set [41]. We evaluate $\psi(2S) \to J/\psi$ feeddown assuming $p_{T,\psi(2S)}/p_{T,J/\psi} = m_{\psi(2S)}/m_{J/\psi} = 1.19$ [42]. The $\chi_{cJ} \to J/\psi$ feeddown contributions are estimated for J/ψ hadroproduction by interpolating ATLAS data [43], and for $J/\psi + Z$ production to be 20% of the direct ${}^3S_1^{[8]}$ production channel, based on Ref. [12] and the fitted value of $\langle \mathcal{O}^{\chi_{c0}}({}^3S_1^{[8]})\rangle$ in Ref. [44]. We neglect χ_{cJ} feeddowns for our polarization predictions due to their small influence on λ_θ [4], and in γp and $\gamma\gamma$ scattering due to their smallness there [27–29]. $\chi_{bJ} \to \Upsilon(nS)$ feeddowns are estimated by using the LHCb measured feeddown fractions [45]. $h_c \to \eta_c$ feeddown is again negligible [11] and neglected, too. We adopt the values for all branching fractions from Ref. [42]. Our fits are standard least-square fits of the three parameters $\langle \mathcal{O}^{J/\psi}({}^3S_1^{[8]})\rangle$, $\langle \mathcal{O}^{J/\psi}({}^1S_0^{[8]})\rangle$ and $\langle \mathcal{O}^{J/\psi}({}^3P_0^{[8]})\rangle/m_c^2$, in this order, taking into account experimental errors and a global 30% theory error due to unknown relativistic corrections. We relate our fit parameters to the three η_c CO LDMEs via HQSS relations [1], and to the $\psi(2S)$ and $\Upsilon(nS)$ CO LDMEs according to the pNRQCD derived relations (3.47)–(3.48) of Ref. [4], where, however, instead of (3.47b) we use its $1/\beta_0$ expanded form up to $O(1/\beta_0)$. The CS LDMEs are not fitted, but fixed as $\langle \mathcal{O}^{J/\psi}({}^3S_1^{[1]})\rangle = 1.16$ GeV^3 [46], $\langle \mathcal{O}^{\psi(2S)}({}^3S_1^{[1]})\rangle = 0.76$ GeV^3 [46], $\langle \mathcal{O}^{\Upsilon(3S)}({}^3S_1^{[1]})\rangle = 3.54$ GeV^3 [46], and $\langle \mathcal{O}^{\eta_c}({}^1S_0^{[1]})\rangle = 0.328$ GeV^3 [47].

TABLE I. Fit results in units of 10^{-2} GeV^3 for our three scale choices $\mu_r = \mu_f = m_T/2$, m_T, and $2m_T$.

$\mu_r = \mu_f$	$\langle \mathcal{O}^{J/\psi}({}^3S_1^{[8]})\rangle$	$\langle \mathcal{O}^{J/\psi}({}^1S_0^{[8]})\rangle$	$\frac{\langle \mathcal{O}^{J/\psi}({}^3P_0^{[8]})\rangle}{m_c^2}$	$\frac{\chi^2_{\rm min}}{\rm d.o.f}$
$m_T/2$	0.592 ± 0.057	-0.205 ± 0.196	0.697 ± 0.089	0.34
m_T	1.050 ± 0.121	0.068 ± 0.2489	1.879 ± 0.261	0.22
$2m_T$	1.382 ± 0.189	0.358 ± 0.303	3.270 ± 0.533	0.21

Fit results. The best-fit values and the χ^2_{min} per degree of freedom (d.o.f.) of our three fits are listed in Table I. The respective correlation matrices are

$$C_{m_T/2} = \begin{pmatrix} 0.323 & -0.360 & 0.498 \\ -0.360 & 3.844 & -0.485 \\ 0.498 & -0.485 & 0.789 \end{pmatrix} \times 10^{-6}\,\text{GeV}^6, \quad (1)$$

$$C_{m_T} = \begin{pmatrix} 1.470 & -0.918 & 3.158 \\ -0.918 & 6.143 & -1.835 \\ 3.158 & -1.835 & 6.838 \end{pmatrix} \times 10^{-6}\,\text{GeV}^6, \quad (2)$$

$$C_{2m_T} = \begin{pmatrix} 3.577 & -1.895 & 10.053 \\ -1.895 & 9.157 & -5.077 \\ 10.053 & -5.077 & 28.376 \end{pmatrix} \times 10^{-6}\,\text{GeV}^6. \quad (3)$$

In Fig. 1, we compare the theoretical predictions using our fit results to the 42 data points. The central values are drawn by solid black lines and the uncertainties by colored bands, whereby the overall uncertainties, as described in the last paragraph of section *Introduction and Overview*, are given by the yellow bands and the uncertainties only of the central fit by the orange bands inside them. We will use this convention for all plots throughout this publication. The level of agreement to the data apparent from Fig. 1 is in line with the very low values of $\chi^2_{\text{min}}/\text{d.o.f.}$ in Table I. The Fock state decomposition shows the familiar features [16,17] of the high p_T J/ψ and η_c fit: On the one hand, it is based on the cancellation between a large positive $^3S_1^{[8]}$ and a large negative $^3P_J^{[8]}$ J/ψ production channel. We note here that this cancellation is not a fine-tuning problem, because NLO LDME mixing implies that only the sum of both contributions has physical significance, see, e.g., Sec. 3.2 of Ref. [36] for more details. On the other hand, $\langle \mathcal{O}^{J/\psi}(^1S_0^{[8]}) \rangle \approx \langle \mathcal{O}^{\eta_c}(^3S_1^{[8]}) \rangle$ is almost solely determined via η_c production: With η_c data already exhausted by the CS contribution, $\langle \mathcal{O}^{J/\psi}(^1S_0^{[8]}) \rangle$ is restricted to very small values.

Prediction of J/ψ polarization. Figures 2(a) and 2(b) show our predictions for the J/ψ polarization parameter λ_θ in the helicity frame, compared to CMS [48,49] and LHCb [50] data. Our predictions are in good agreement with these measurements and match the pattern that λ_θ turns from slightly negative at relatively low p_T to positive and converges to $\lambda_\theta \sim 0.3$ at high p_T. No J/ψ polarization puzzle appears here.

Prediction of J/ψ hadroproduction at very high p_T. The recent ATLAS measurement [26] of the J/ψ p_T differential distribution at $\sqrt{s} = 13$ TeV with p_T ranging up to 360 GeV, which we compare our predictions to in Fig. 2(c), has received significant attention. In the publication itself, data was compared to NLO NRQCD predictions using LDME input from Ref. [10]. Although there were no unreasonable discrepancies, theory errors were expectedly large at these very high p_T values with their dominating $\log(m_c^2/p_T^2)$ terms. This effect depends however on the LDME set chosen. We can fortunately infer a negligible effect on our results from Fig. 3 of Ref. [53], where the *resummed* curve of the Chao *et al.* [16] LDMEs panel describes the ATLAS data [26] well, noticing that the LDMEs of Ref. [16] do not significantly differ from our default LDMEs.

Prediction of J/ψ hadroproduction at low p_T. In Fig. 2(d), we compare our predictions to J/ψ production data from LHCb [51], reaching down to $p_T = 1$ GeV. Here, we recover the feature familiar from other high p_T fits [3,4,14–18] that low p_T data is not reproduced. The reason is that the $^3P_J^{[8]}$ SDCs change sign from negative to positive when going below $p_T \approx 7$ GeV, so that instead of a cancellation between $^3S_1^{[8]}$ and $^3P_J^{[8]}$ channels there is an amplification. The resulting steep increase at low p_T is not observed in the data.

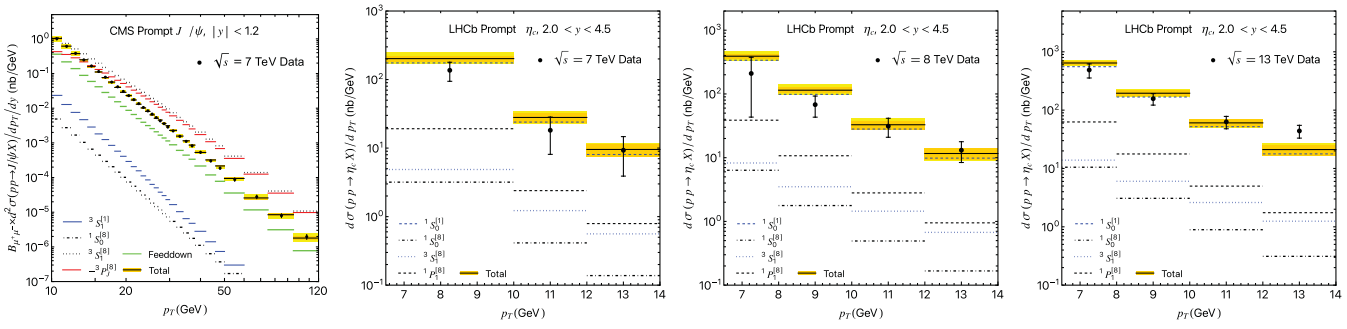


FIG. 1. Predictions for prompt J/ψ production at CMS [25] and η_c production at LHCb [23,24]. The data shown is exactly the data used for the LDME fits. The total cross section is broken down into feeddown contributions and the direct contributions of the individual Fock states. The orange bands describe the uncertainties from the fit correlations without considering scale variations. The yellow bands include the effect of both fit correlations and scale variations as described in the last paragraph of section *Introduction and overview*.

Prediction of $\Upsilon(3S)$ hadroproduction. Figure 2e shows our predictions for the p_T differential $\Upsilon(3S)$ production measured by ATLAS [30]. These results are a genuine prediction of the equations (3.47)–(3.48) of Ref. [4] derived from pNRQCD, which relate $\Upsilon(3S)$ to the J/ψ CO LDMEs. The accurate description seen in Fig. 2(e) can thus also be viewed as a highly nontrivial confirmation of the pNRQCD relations, the more so as scale evolutions in Eq. (3.47) of Ref. [4] result in a very different Fock state decomposition in $\Upsilon(3S)$ as compared to J/ψ production. In particular, there is no strong cancellation between $^3S_1^{[8]}$ and $^3P_J^{[8]}$ channels here. Instead, the cross section decomposes almost equally into the $^3S_1^{[8]}$ channel and feeddown from χ_{bJ} mesons. For $\Upsilon(1S)$ and $\Upsilon(2S)$, we reach similar conclusions.

Prediction of LHCb $J/\psi + Z$ production. In Fig. 2(f), we show our predictions for $J/\psi + Z$ production measured by ATLAS [21], where estimated double parton scattering (DPS) contributions are already subtracted from the data. The predictions are dominated by the $^3S_1^{[8]}$ channel. For the two highest p_T bins, predictions lie around two experimental standard deviations below data. Given the fact that in Ref. [21], a data-driven analysis of the J/ψ-Z angular distribution confirmed single parton scattering

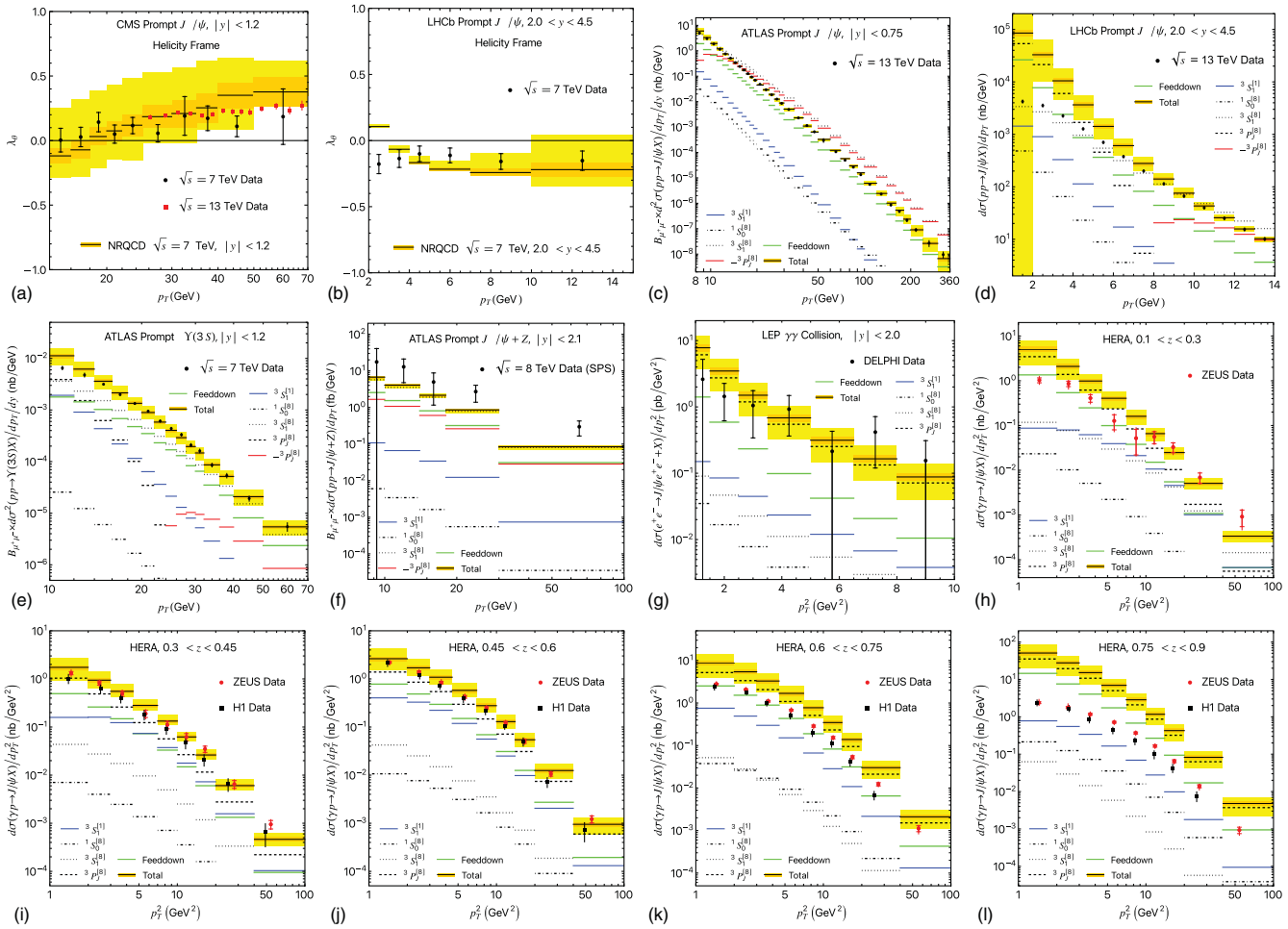


FIG. 2. Theory predictions for the J/ψ polarization parameter λ_θ in the helicity frame compared to CMS [48,49] (a) and LHCb [50] (b) data, for J/ψ hadroproduction measured by ATLAS [26] (c) and LHCb [51] (d), for $\Upsilon(3S)$ [30] (e) and $J/\psi + Z$ [21] (f) production measured by ATLAS, for LEP DELPHI two photon collision data [27] (g), and for HERA H1 [28] and ZEUS [29] photoproduction data (h)–(l). For the $J/\psi + Z$ data shown in the plot, we have assumed $\sigma(pp \to Z + X) = (33.14 \pm 1.19)$ nb as in Ref. [12], and subtracted the DPS contributions estimated in Ref. [21] using the DPS effective area value $\sigma_{\rm eff} = 15^{+5.8}_{-4.2}$ mb of Ref. [52]. The $J/\psi + Z$ data is subtracted by the DPS contributions estimated in Ref. [21] using the DPS effective area value $\sigma_{\rm eff} = 15^{+5.8}_{-4.2}$ mb of Ref. [52]. To compare with the HERA γp data, we use ZEUS [29] kinematics and divide the calculated e^+e^- cross sections by the averaged photon flux 0.1024 [28]. Panels (g) to (l) show the sum of non-, single-, (and double-)resolved photon contributions, which are not broken down here, to avoid clutter. In all panels, the total cross sections are broken down into feeddown contributions and the direct contributions of the individual Fock states. The orange bands describe the uncertainties from the fit correlations without considering scale variations. The yellow bands include the effect of both fit correlations and scale variations as described in the last paragraph of section *Introduction and overview*.

(SPS) dominance, it appears unlikely, albeit not impossible, that the discrepancy is due to underestimated DPS contributions. This conclusion is however based on the assumption that the pocket formula underlying the ATLAS DPS estimation holds, which itself is, however, subject to debate.

Prediction of J/ψ production in $\gamma\gamma$ scattering. In Fig. 2(g), we show predictions for p_T^2 differential J/ψ production in $\gamma\gamma$ scattering at LEP DELPHI [27], in the range $1\ \mathrm{GeV}^2 < p_T^2 < 10\ \mathrm{GeV}^2$. Contrary to the hadroproduction case, this low p_T data is reasonably well described, even though the very low statistics of the measurement does not allow for more than an order-of-magnitude comparison. We note that the cross sections are almost exclusively given by single-resolved photon contributions.

Predictions of J/ψ production in HERA photoproduction. In Figs. 2(h)–2(l), we show our predictions for p_T^2 differential J/ψ photoproduction at HERA [28,29] for five bins of the inelasticity variable z, which measures in the proton rest frame the fraction of photon energy transferred to the J/ψ. In the region $0.1 < z < 0.3$ with $p_T^2 < 40\ \mathrm{GeV}^2$, resolved photons are dominating our predictions, while for the other regions, nonresolved photons are dominating. We recover the increase of the cross section at $z \to 1$, known, e.g., from Fig. 3.3 of Ref. [54], which is not observed in the data. For $0.75 < z < 0.9$, predictions overshoot the data by factors of 5.2 to 20. Surprisingly, in the $z < 0.6$ regions, we obtain a good description of the data over the whole measured p_T range, again down to $p_T = 1$ GeV, with a significant deviation only for the low p_T end of the lowest z bin, which coincides with the region where resolved photoproduction dominates.

Discussion. Although NLO predictions of the high p_T J/ψ plus η_c combined fit presented here lead to many nontrivial descriptions of various quarkonium production data, discrepancies remain. Moreover, these discrepancies are not at places where one would naively expect them. A naive expectation would be that fixed order NLO calculations may fail at $p_T^2 \gg 4m_Q^2$ and in the endpoint regions $p_T^2 \ll 4m_Q^2$ and $1 - z \ll 1$, where large logarithms spoil the perturbative convergence. The hadroproduction predictions from the LDME fit presented here are, however, very good for $p_T^2 \gg 4m_Q^2$, and fail only in the region $p_T^2 \lessapprox 4m_Q^2$. On the other hand, the latter region works well for $z < 0.6$ HERA photoproduction, while for $z > 0.6$, HERA data is not described, regardless of p_T. LDME universality thus remains in question. However, as pointed out above, we could find indications from Ref. [53] that, for our LDMEs, resummations in the large p_T hadroproduction limit would yield no large effect. Furthermore, it is noticeable that the remaining regions of disagreement, $p_T^2 \lessapprox 4m_Q^2$ in hadroproduction and $z > 0.6$ in photoproduction, coincide with extensions of endpoint regions, for which solutions, e.g., via small-x resummation [55] and nonperturbative shape functions [56,57], have been proposed. This is also true for the BELLE cross section $e^+e^- \to J/\psi + X_{\mathrm{non}\,c\bar{c}}$ [58], see Refs. [56,59], where we have tested that using the SDCs from Ref. [59] and our default fit LDMEs, we obtain a good description of the BELLE data.

Summary. To summarize, we have done a combined fit of the three J/ψ CO LDMEs to 42 data points of CMS J/ψ and LHCb η_c production data and made predictions for CMS and LHCb J/ψ polarization, ATLAS high p_T J/ψ production, ATLAS $\Upsilon(3S)$ and $J/\psi + Z$ production, LHCb low p_T J/ψ production as well as J/ψ production in $\gamma\gamma$ collisions at LEP and γp collisions at HERA. We have thereby used a novel fit-and-predict procedure, which systematically takes into account the effect of scale variations. The predictions show good agreement with data everywhere with the exception of low and medium p_T hadroproduction, HERA photoproduction at $z > 0.6$, and possibly the two highest LHCb $J/\psi + Z$ production bins. In particular, our findings for J/ψ production in $\gamma\gamma$ and γp scattering may be of significance for future quarkonium studies, in particular at the EIC and the high-luminosity LHC.

Acknowledgments. X.-P. W would like to thank A. Bruni, Y.-Q. Ma, and H.-S Shao for useful discussions. We thank A. Vairo for reading the paper and giving very useful comments. The work of N. B. and X.-P. W. is supported by the DFG (Deutsche Forschungsgemeinschaft, German Research Foundation) Grant No. BR 4058/2-2. We acknowledge support from the DFG cluster of excellence "ORIGINS" under Germany's Excellence Strategy—EXC-2094-390783311. X.-P. W. acknowledges support from STRONG-2020- European Union's Horizon 2020 research and innovation program under Grant Agreement No. 824093. N. B. acknowledges the European Union ERC-2023-ADG- Project EFT-XYZ. The work of X.-P. W. is supported by the National Natural Science Foundation of China under Grant No. 12135006. The work of M. B. is supported by the German Research Foundation DFG through Grant No. BU 3455/1-1 as part of the Research Unit FOR2926. The authors would like to express special thanks to the Mainz Institute for Theoretical Physics (MITP) of the Cluster of Excellence PRISMA+ (Project ID 390831469) for its hospitality and support.

[1] G. T. Bodwin, E. Braaten, and G. P. Lepage, Rigorous QCD analysis of inclusive annihilation and production of heavy quarkonium, Phys. Rev. D **51**, 1125 (1995); **55**, 5853(E) (1997).

[2] G. P. Lepage, L. Magnea, C. Nakhleh, U. Magnea, and K. Hornbostel, Improved nonrelativistic QCD for heavy quark physics, Phys. Rev. D **46**, 4052 (1992).

[3] N. Brambilla, H. S. Chung, A. Vairo, and X.-P. Wang, Production and polarization of S-wave quarkonia in potential nonrelativistic QCD, Phys. Rev. D **105**, L111503 (2022).

[4] N. Brambilla, H. S. Chung, A. Vairo, and X.-P. Wang, Inclusive production of J/ψ, ψ(2S), and Υ states in pNRQCD, J. High Energy Phys. 03 (**2023**) 242.

[5] A. Pineda and J. Soto, Effective field theory for ultrasoft momenta in NRQCD and NRQED, Nucl. Phys. B, Proc. Suppl. **64**, 428 (1998).

[6] N. Brambilla, A. Pineda, J. Soto, and A. Vairo, Potential NRQCD: An effective theory for heavy quarkonium, Nucl. Phys. **B566**, 275 (2000).

[7] N. Brambilla, A. Pineda, J. Soto, and A. Vairo, Effective field theories for heavy Quarkonium, Rev. Mod. Phys. **77**, 1423 (2005).

[8] N. Brambilla, H. S. Chung, and A. Vairo, Inclusive hadroproduction of P-Wave heavy quarkonia in potential nonrelativistic QCD, Phys. Rev. Lett. **126**, 082003 (2021).

[9] N. Brambilla, H. S. Chung, and A. Vairo, Inclusive production of heavy quarkonia in pNRQCD, J. High Energy Phys. 09 (2021) 032.

[10] M. Butenschoen and B. A. Kniehl, World data of J/ψ production consolidate NRQCD factorization at NLO, Phys. Rev. D **84**, 051501 (2011).

[11] M. Butenschoen, Z.-G. He, and B. A. Kniehl, η_c production at the LHC challenges nonrelativistic-QCD factorization, Phys. Rev. Lett. **114**, 092004 (2015).

[12] M. Butenschoen and B. A. Kniehl, Constraints on nonrelativistic-qcd long-distance matrix elements from J/ψ plus W/Z production at the LHC, Phys. Rev. Lett. **130**, 041901 (2023).

[13] M. Butenschoen and B. A. Kniehl, J/ψ polarization at tevatron and LHC: Nonrelativistic-QCD factorization at the crossroads, Phys. Rev. Lett. **108**, 172002 (2012).

[14] Y.-Q. Ma, K. Wang, and K.-T. Chao, $J/\psi(\psi')$ production at the tevatron and LHC at $\mathcal{O}(\alpha_s^4 v^4)$ in nonrelativistic QCD, Phys. Rev. Lett. **106**, 042002 (2011).

[15] B. Gong, L.-P. Wan, J.-X. Wang, and H.-F. Zhang, Polarization for prompt J/ψ and ψ(2s) production at the tevatron and LHC, Phys. Rev. Lett. **110**, 042002 (2013).

[16] H. Han, Y.-Q. Ma, C. Meng, H.-S. Shao, and K.-T. Chao, η_c production at LHC and indications on the understanding of J/ψ production, Phys. Rev. Lett. **114**, 092005 (2015).

[17] H.-F. Zhang, Z. Sun, W.-L. Sang, and R. Li, Impact of η_c hadroproduction data on charmonium production and polarization within NRQCD framework, Phys. Rev. Lett. **114**, 092006 (2015).

[18] G. T. Bodwin, K.-T. Chao, H. S. Chung, U.-R. Kim, J. Lee, and Y.-Q. Ma, Fragmentation contributions to hadroproduction of promptJ/ψ, χ_{cJ}, and $\psi(2S)$ states, Phys. Rev. D **93**, 034041 (2016).

[19] M. Butenschoen and B. A. Kniehl, Next-to-leading-order tests of NRQCD factorization with J/ψ yield and polarization, Mod. Phys. Lett. A **28**, 1350027 (2013).

[20] G. Aad *et al.* (ATLAS Collaboration), Measurement of the production cross section of prompt J/ψ mesons in association with a $W^{\pm}$ boson in pp collisions at $\sqrt{s} =$ 7 TeV with the ATLAS detector, J. High Energy Phys. 04 (2014) 172.

[21] G. Aad *et al.* (ATLAS Collaboration), Observation and measurements of the production of prompt and non-prompt J/ψ mesons in association with a Z boson in pp collisions at $\sqrt{s} = 8$ TeV with the ATLAS detector, Eur. Phys. J. C **75**, 229 (2015).

[22] M. Aaboud *et al.* (ATLAS Collaboration), Measurement of J/ψ production in association with a $W^{\pm}$ boson with pp data at 8 TeV, J. High Energy Phys. 01 (2020) 095.

[23] R. Aaij *et al.* (LHCb Collaboration), Measurement of the $\eta_c(1S)$ production cross-section in proton-proton collisions via the decay $\eta_c(1S) \to p\bar{p}$, Eur. Phys. J. C **75**, 311 (2015).

[24] R. Aaij *et al.* (LHCb Collaboration), Study of charmonium production via the decay to $p\bar{p}$ at $\sqrt{s} = 13$TeV, Eur. Phys. J. C **84**, 1274 (2024).

[25] V. Khachatryan *et al.* (CMS Collaboration), Measurement of J/ψ and ψ(2S) prompt double-differential cross sections in pp collisions at $\sqrt{s} = 7$ TeV, Phys. Rev. Lett. **114**, 191802 (2015).

[26] G. Aad *et al.* (ATLAS Collaboration), Measurement of the production cross-section of J/ψ and $\psi(2S)$ mesons in pp collisions at $\sqrt{s} = 13$ TeV with the ATLAS detector, Eur. Phys. J. C **84**, 169 (2024).

[27] J. Abdallah *et al.* (DELPHI Collaboration), Study of inclusive J/ψ production in two photon collisions at LEP-2 with the DELPHI detector, Phys. Lett. B **565**, 76 (2003).

[28] F. D. Aaron *et al.* (H1 Collaboration), Inelastic production of J/ψ mesons in photoproduction and deep inelastic scattering at HERA, Eur. Phys. J. C **68**, 401 (2010).

[29] H. Abramowicz *et al.* (ZEUS Collaboration), Measurement of inelastic J/ψ and ψ' photoproduction at HERA, J. High Energy Phys. 02 (2013) 071.

[30] G. Aad *et al.* (ATLAS Collaboration), Measurement of upsilon production in 7 TeV pp collisions at ATLAS, Phys. Rev. D **87**, 052004 (2013).

[31] M. Butenschoen and B. A. Kniehl, Global analysis of ψ(2S) inclusive hadroproduction at next-to-leading order in nonrelativistic-QCD factorization, Phys. Rev. D **107**, 034003 (2023).

[32] M. Butenschoen and B. A. Kniehl, Probing nonrelativistic QCD factorization in polarized J/ψ photoproduction at next-to-leading order, Phys. Rev. Lett. **107**, 232001 (2011).

[33] M. Butenschoen and B. A. Kniehl, Reconciling J/ψ production at HERA, RHIC, Tevatron, and LHC with NRQCD factorization at next-to-leading order, Phys. Rev. Lett. **106**, 022003 (2011).

[34] M. Butenschoen, Z.-G. He, and B. A. Kniehl, Deciphering the $X(3872)$ via its polarization in prompt production at the CERN LHC, Phys. Rev. Lett. **123**, 032001 (2019).

[35] M. Butenschoen, Z.-G. He, and B. A. Kniehl, NLO NRQCD disfavors the interpretation of X(3872) as $\chi_{c1}(2P)$, Phys. Rev. D **88**, 011501 (2013).
[36] M. Butenschoen and B. A. Kniehl, Dipole subtraction at next-to-leading order in nonrelativistic-QCD factorization, Nucl. Phys. **B950**, 114843 (2020).
[37] M. Butenschoen and B. A. Kniehl, Dipole subtraction vs. phase space slicing in NLO NRQCD heavy-quarkonium production calculations, Nucl. Phys. **B957**, 115056 (2020).
[38] B. W. Harris and J. F. Owens, The Two cutoff phase space slicing method, Phys. Rev. D **65**, 094032 (2002).
[39] M. Butenschoen and B. A. Kniehl, Complete next-to-leading-order corrections to J/ψ photoproduction in nonrelativistic quantum chromodynamics, Phys. Rev. Lett. **104**, 072001 (2010).
[40] J. Pumplin, D. R. Stump, J. Huston, H. L. Lai, P. M. Nadolsky, and W. K. Tung, New generation of parton distributions with uncertainties from global QCD analysis, J. High Energy Phys. 07 (2002) 012.
[41] P. Aurenche, M. Fontannaz, and J. P. Guillet, New NLO parametrizations of the parton distributions in real photons, Eur. Phys. J. C **44**, 395 (2005).
[42] S. Navas *et al.* (Particle Data Group), Review of particle physics, Phys. Rev. D **110**, 030001 (2024).
[43] G. Aad *et al.* (ATLAS Collaboration), Measurement of χ_{c1} and χ_{c2} production with $\sqrt{s} = 7$ TeV pp collisions at ATLAS, J. High Energy Phys. 07 (2014) 154.
[44] Y.-Q. Ma, K. Wang, and K.-T. Chao, QCD radiative corrections to χ_{cJ} production at hadron colliders, Phys. Rev. D **83**, 111503 (2011).
[45] R. Aaij *et al.* (LHCb Collabortaion), Study of χ_b meson production in p p collisions at $\sqrt{s} = 7$ and 8 TeV and observation of the decay $\chi_b(3P) \to \Upsilon(3S)\gamma$, Eur. Phys. J. C **74**, 3092 (2014).
[46] E. J. Eichten and C. Quigg, Quarkonium wave functions at the origin, Phys. Rev. D **52**, 1726 (1995).
[47] G. T. Bodwin, H. S. Chung, D. Kang, J. Lee, and C. Yu, Improved determination of color-singlet nonrelativistic QCD matrix elements for S-wave charmonium, Phys. Rev. D **77**, 094017 (2008).
[48] S. Chatrchyan *et al.* (CMS Collaboration), Measurement of the prompt J/ψ and $\psi(2S)$ Polarizations in pp collisions at $\sqrt{s} = 7$ TeV, Phys. Lett. B **727**, 381 (2013).
[49] A. Hayrapetyan *et al.* (CMS Collaboration), Measurement of the polarizations of prompt and non-prompt Image 1 and $\psi(2S)$ mesons produced in pp collisions at $s = 13$TeV, Phys. Lett. B **858**, 139044 (2024).
[50] R. Aaij *et al.* (LHCb Collaboration), Measurement of J/ψ polarization in pp collisions at $\sqrt{s} = 7$ TeV, Eur. Phys. J. C **73**, 2631 (2013).
[51] R. Aaij *et al.* (LHCb Collaboration), Measurement of forward J/ψ production cross-sections in pp collisions at $\sqrt{s} = 13$ TeV, J. High Energy Phys. 10 (2015) 172; 05 (2017) 63(E).
[52] G. Aad *et al.* (ATLAS Collaboration), Measurement of hard double-parton interactions in $W(\to l\nu)$+ 2 jet events at $\sqrt{s} = 13$ TeV with the ATLAS detector, New J. Phys. **15**, 033038 (2013).
[53] H. S. Chung, U.-R. Kim, and J. Lee, Resummation of threshold double logarithms in hadroproduction of heavy quarkonium, Phys. Rev. Lett. **134**, 071902 (2025).
[54] D. Boer *et al.*, Physics case for quarkonium studies at the electron ion collider, Prog. Part. Nucl. Phys. **142**, 104162 (2025).
[55] Y.-Q. Ma and R. Venugopalan, Comprehensive description of J/ψ production in proton-proton collisions at collider energies, Phys. Rev. Lett. **113**, 192301 (2014).
[56] M. Beneke, I. Z. Rothstein, and M. B. Wise, Kinematic enhancement of nonperturbative corrections to quarkonium production, Phys. Lett. B **408**, 373 (1997).
[57] S. Fleming, A. K. Leibovich, and T. Mehen, Resummation of large endpoint corrections to color-octet J/ψ photoproduction, Phys. Rev. D **74**, 114004 (2006).
[58] P. Pakhlov *et al.* (Belle Collaboration), Measurement of the cross section for exclusive $e^+ e^- \to D^{(*)\pm} D^{*\mp}$ production at $\sqrt{S} = 10.58$ GeV, Phys. Rev. D **79**, 071101 (2009).
[59] A.-P. Chen, X.-B. Jin, Y.-Q. Ma, and C. Meng, Color-octet contributions for J/ψ inclusive production at B factories in soft gluon factorization, J. High Energy Phys. 03 (2022) 202.